Inorganic Chemistry

Article

pubs.acs.org/IC

Selective Lability of Ruthenium(II) Arene Amino Acid Complexes

Tom G. Scrase,[†] Michael J. O'Neill,[†] Andrew J. Peel, Paul W. Senior, Peter D. Matthews, Heyao Shi,[‡] Sally R. Boss,* and Paul D. Barker*

University of Cambridge, Chemistry Department, Lensfield Road, Cambridge CB2 1EW, United Kingdom

Supporting Information

ABSTRACT: A series of organometallic complexes of the form [(PhH)Ru-(amino acid)]$^+$ have been synthesized using amino acids able to act as tridentate ligands. The straightforward syntheses gave enantiomerically pure complexes with two stereogenic centers due to the enantiopurity of the chelating ligands. Complexes were characterized in the solid-state and/or solution-state where the stability of the complex allowed. The propensity toward labilization of the coordinatively saturated complexes was investigated. The links between complex stability and structural features are very subtle. Nonetheless, H/D exchange rates of coordinated amino groups reveal more significant differences in reactivity linked to metallocycle ring size resulting in decreasing stability of the metallocycle as the amino acid side-chain length increases. The behavior of these systems in acid is unusual, apparently labilizing the carboxylate residue of the amino acid. This acid-catalyzed hemilability in an organometallic is relevant to the use of Ru(II) arenes in medicinal contexts due to the relatively low pH of cancerous cells.

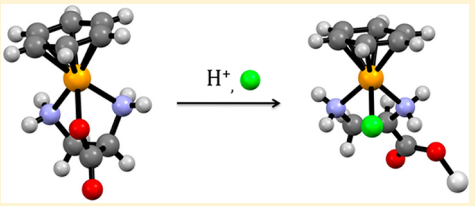

INTRODUCTION

Ruthenium arene complexes have been studied extensively for their potential as medicinal compounds, particularly for their anticancer properties.[1−6] Evidence is accumulating that ruthenium complexes with labile ligands are relatively promiscuous and the speciation observed when such complexes are challenged with complex biological solutions is extensive.[7,8,6] Given the abundance of different Lewis basic groups on polypeptides, nucleic acids, and even small metabolites, this is not surprising. Consequently, establishing the link between ligand exchange properties and cytotoxicity remains a challenge, although there is already extensive literature which charts the cytotoxicities of chemically diverse ruthenium species.

An advantage of incorporating metals into complexes that could be thought of as drug candidates comes from the inherent strength of the resulting coordination bonds that could form between the complex and any given target. However, delivering complexes with labile ligands results in promiscuous binding to biomolecules and hence lack of selectivity, which is an undesirable characteristic in a drug. Relatively simple ruthenium(III) coordination complexes, such as NAMI-A and KP1019, fall into this category. Both initially showed some promise as anticancer compounds, but their modes of action have been difficult to define because the chemical fates of these labile complexes cannot be determined. At the other end of the spectrum Meggers et al. exploited inert metal complexes simply as structural platforms able to extend the valency space available to medicinal chemists beyond carbon.[9,10] In between these extremes, Sadler[11,12] and Dyson[1,13] in particular have independently explored ruthenium-(II) complexes with limited (one or two) labile coordination sites.

In this article, we present the synthesis and characterization of a series of novel Ru(II) arene complexes, together with some pertinent investigations into their reactivity. The complexes under study exclusively incorporate chelating ligands. The use of chelating ligands in these complexes will restrict their promiscuity by slowing any ligand substitutions which will, we believe, allow for a degree of selectivity in binding.

In order to synthesize chelates with appreciable opportunity for selectivity, we decided to use amino acids as a cheap and plentiful source of multidentate, chiral ligands. Consideration of the different ways that mono- or bidentate ligands could bind (and the consequences for the configuration of the metal center) led us to use amino acids able to act as tridentate ligands in order to "lock-in" the stereochemistry of the metal center (Scheme 1). This approach has the additional benefit of ligand sets which would likely act in a hemilabile manner, allowing fine control over ligand exchange rates. We note that

Scheme 1. Generalized Structure of the Tridentate Amino Acid Cations with the Ruthenium(II) Arene Unit[a]

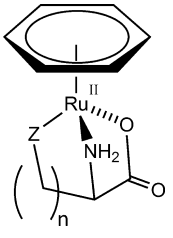

[a] n is the number of CH_2 groups between the amino acid α carbon and the coordinating atom provided by the side-chain. Values of n for the different amino acids and the cation identification numbers are recorded in Table 1.

Received: August 26, 2014
Published: March 23, 2015

DOI: 10.1021/ic502051y
Inorg. Chem. 2015, 54, 3118−3124

others have recently examined reactions of the ruthenium(II) arene unit with selected amino acids and the cytotoxicity of some specific compounds, but these compounds have neither been extensively characterized nor systematically varied.[14−16] Additionally, some complexes with arenes functionalized with pendant amines,[17] including phenylalanine,[18] which contain a different class of chelating ligand, have been studied. The reaction of some of these with DNA has been examined.[17]

The effect of the chelate ring size in such complexes has not been studied in detail and certainly not in the context of amino acid coordination. As shown below, this strongly influences the stability of the chelate, the properties of coordinating ligand groups, and hence the selective lability of the whole complex.

Our long-term aim is to use our understanding of this molecular behavior to rationally design ruthenium drug candidates with tunable binding lifetimes due to the unique and orthogonal coordination chemistry of the metal. From this we can learn how to attenuate the ligand exchange rates of what are expected to be very stable complexes. This current work therefore addresses the fundamental inorganic chemistry underpinning our strategy for medicinal studies.

RESULTS AND DISCUSSION

A number of related complexes containing the $[(PhH)Ru]^{2+}$ unit and amino acids have been synthesized and characterized, exploiting the enantiopurity of the amino acid feedstock to limit the diastereomeric outcome of the synthesis. Such complexes are predicted to be classically inert, being chelates of a low-spin $4d^6$ metal center with no obviously labile ligand.

The structure of these complexes may be described as a half-sandwich ruthenium complex formed by the coordination of a benzene ligand and a tridentate amino acidate ligand (Scheme 1). Coordination of the tridentate amino acidate ligand produces a fused-metallocyclic motif with the ligands under discussion here. Varying the side-chain length of the ligand should alter the characteristics of the fused metallocycle. Due to the use of naturally occurring amino acids as ligands, coordination of the α-amino and carboxylate groups produces a 5-membered metallocycle common to all of these complexes. With the benzene ligand also being conserved across this series of complexes, the general structure possesses two features that can be systematically varied: the amino acid side-chain length, n, and the identity of the side-chain functional group, Z. (see Scheme 1 and Table 1).

Table 1. Summary of the Tridentate Amino Acid Complexes under Investigation and the Generalized Structure of the Cations, [(PhH)Ru(amino acid)]$^{+a}$

cation	amino acid	n	side-chain functional group (Z)
1	L-2,3-diamino-propionic acid (DAP)	1	NH_2
2	L-2,4-diamino-butanoic acid (DAB)	2	NH_2
3	L-ornithine	3	NH_2
4	L-lysine	4	NH_2
5	L-histidine	2	imidazole
6	L-methionine	2	SMe
7^b	L-aspartate	2	COO^-

[a]We use the complex identifiers (bold numbers in the text) to refer to the monovalent cation. They have all been synthesized as the $[PF_6]^-$ salt. [b]**7** is a neutral complex.

One rationale behind the particular suite of complexes chosen was simply to vary the metallocyclic ring size systematically. **1**, **2**, **5**, and **6** were successfully synthesized, purified, and crystallized such that high resolution structures could be obtained. Despite significant effort, complex **3** has not crystallized, but we have successfully characterized its structure in solution using NMR spectroscopy (see below and Supporting Information section 1). To date, we have been unable to isolate complex **4**, but it can be detected by ESI-MS in reaction mixtures. Complex **7** has been characterized in solution only. (See Supporting Information section 1.2.)

In principle, complexation of amino acids in a tridentate fashion as described above should give rise to a minimum of four diastereomers with the metal becoming a new stereocenter. Of course, using enantiomerically pure ligands would result in only two of the diastereomers being possible, but it is clear (Figure 1) that the single enantiomers of the amino acids

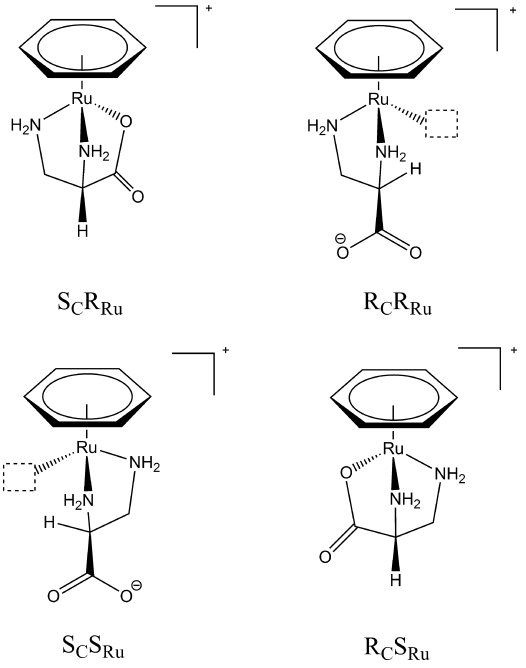

Figure 1. Possible diastereomers of **1** and the absolute configuration at the Cα and Ru centers.

cannot generate a tridentate binding motif with the metal in both the R and S configurations. Hence, using pure L-amino acids results in only one diastereomer with the ruthenium exclusively in the R configuration.

This stereochemistry is exactly what is observed for **1**, **2**, **5**, and **6** both in the solid- and solution-states (Figure 2), and the NMR spectroscopy data collected for **3** are also consistent with this.

Additionally, synthesis of **1** using racemic, D,L-DAP and subsequent X-ray diffraction analysis of the resulting crystals revealed two cations in the unit cell, related to each other by a center of inversion; these are one cation of each diastereomer with configurations S_CR_{Ru} and R_CS_{Ru}, respectively.

The existence of enantiopure products is also apparent in the solution-state. For example, the ^{1}H NMR spectrum of [**1**][PF_6] shows that the methylene group protons are in unique chemical environments. Furthermore, the α-CH group proton couples to both methylene protons with distinct $^3J_{HH}$ coupling constants (see Supporting Information sections 1.2 and 1.3 for full NMR

DOI: 10.1021/ic502051y
Inorg. Chem. 2015, 54, 3118−3124

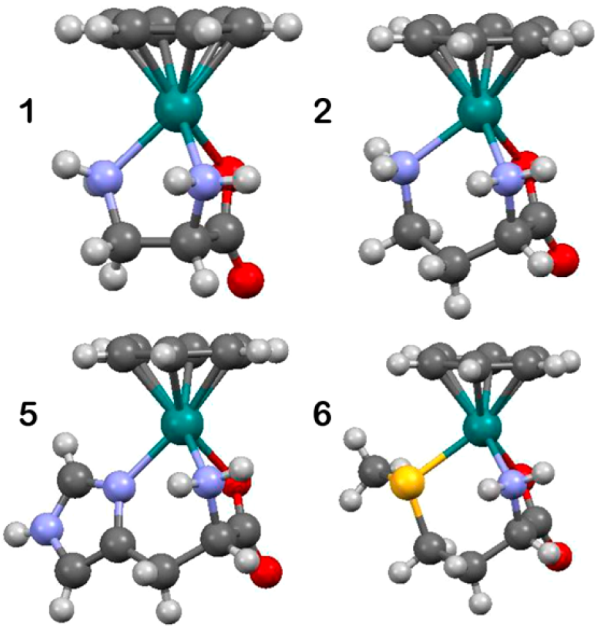

Figure 2. Ball-and-stick representations of the crystal structures of the cations **1**, **2**, **5**, and **6**. H atoms were not resolved, but the calculated positions are shown to aid stereochemical appreciation relevant to our data from NMR spectroscopy.

assignments). The rigidity of the metallocyclic solid-state structure of **1** is, therefore, clearly retained in solution as shown by the nondegeneracy of the protic environments constrained within the chelating ring. As such the methylene and amino group protons are pro-chiral. A combination of one- and two-dimensional methods have enabled us to distinguish between the pro-chiral methlyene protons as well as those attached to the metal coordinated α and side-chain nitrogen atoms (see Supporting Information section 1.3.2).

A similar analysis of [**2**][PF_6] also reveals distinct protic environments for the protons attached to the pro-chiral nitrogen and carbon atoms contained within the metallocycles which indicates that the solid-state structure of this complex is retained in the solution phase.

Interestingly, as well as the C and Ru configurations, a third stereogenic center arises in the case of binding methionine to the $[(PhH)Ru]^{2+}$ synthon. While tridentate L-methionine binds to give the *R*-configuration at Ru, the sulfur center becomes either *R*- or *S*-, depending on the position of the methyl group with respect to the stereochemically active lone pair. We obtained crystals of the complex showing the sulfur center in the *S*-configuration, but computational modeling of the two configurations suggests that they differ in energy *in vacuo* by only 0.050 kcal mol^{-1}. The ^1H NMR spectrum of the product displays two species in a 1:1 ratio, consistent with racemization at the S center. We believe that although we isolated only one species in the crystal, both exist in solution. Whether or not this is due to fluxionality at the sulfur center is unclear from our studies to date.

It is clear that the length of the side-chain plays a significant role in the effectiveness of the coordination of the side-chain. For the complexes we have been able to structurally characterize in detail, **1** and **2**, the differences are subtle. A small increase in Ru−N bond length on going from **1** (2.131(4) Å) to **2** (2.153(3) Å) is observed alongside a large change in the Ru−N−C bond angle for the side-chain amino group (111.8(4)° and 119.3(2)°, respectively). The increasing Ru−N bond length and Ru−N−C bond angle reflect poorer orbital overlap between the amino group lone pair and the vacant metal orbital, reducing the covalent component to the bonding and weakening the metal nitrogen interaction.

While it was not possible to characterize [**3**][PF_6] in the solid-state by X-ray diffraction studies, analysis in the solution-state using both one- and two-dimensional techniques allowed for a proposed conformation of the metallocyclic system in which the pro-chiral protons attached to the α and side-chain nitrogens and the γ and δ carbon atoms can also be resolved (Supporting Information section 1.2). The suggested conformation of the metallocyclic system of **3** in solution is depicted in Figure 3.

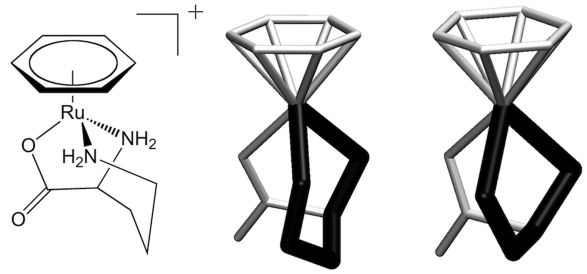

Figure 3. Proposed structure of [**3**] (left) compared to the solid-state structures of [**2**] (middle) and [**1**] (right).

As mentioned above, synthesis and isolation of the tridentate lysine coordinated complex, **4**, has not been successful. A variety of different solvents and anions have been used to try to capture this cation as a salt but without success. NMR spectroscopy and ESI-MS studies have shown a variety of species in the reaction mixtures. The NMR spectra have not been interpretable, but the MS data show that the tridentate species is present (m/z = 325.1 Da, expected 325.0). In addition we also observe species with the lysine coordinated to the ruthenium in a bidentate manner with either a chloride (m/z 361 Da) or water (m/z 342) ligand occupying the remained coordination site of the metal. Two smaller species that we cannot identify (m/z 307 and 262 Da) were also apparent.

Varying the side-chain functional group will clearly impact the structure of the metallocycle which it generates. This can be seen for the complexes **2**, **5**, and **6** for which a 6-membered metallocycle is fixed by the side-chain. Complexes **2** and **6** result in chairlike conformations of this metallocycle while the two sp^2 centers of the imidazole in **5** produce a twist-chairlike conformation (Figure 4).

In keeping with the results for the other metallocyclic structures, an analysis of the solution-state structure of [**5**][PF_6] allows the protons attached to the pro-chiral α

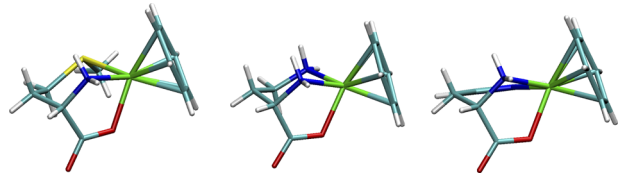

Figure 4. Solid-state structures of complexes **2** (middle), **5** (right), and **6** (left) comparing conformations of 6-membered metallocycles.

DOI: 10.1021/ic502051y
Inorg. Chem. 2015, 54, 3118−3124

nitrogen atom to be distinguished from one another (although in this case the methylene protons appear coincident in the ^{1}H NMR spectra).

Such a thorough analysis of the pro-chiral proton environments within the metallocyclic structures was prompted as a result of observing distinct and, in some cases, significantly different H−D proton exchange rates for the coordinated NH protons, further demonstrating their chemical inequivalence. We sought to investigate whether these rates of exchange could be correlated with the strength of the coordination bond formed between the metal and the amine in the hope that these exchange rates might find use as "reporters" for the strength and reactivity of the metal−nitrogen bonds contained in the complexes. The results are presented in Table 2. The resonance of the γ-NH_{proR} of **2** is very close to the water signal, and this precludes accurate measurement of its rate of exchange in buffered D_2O.

Table 2. Observed First-Order Rate Constants (s^{-1}) for H−D Exchange of Amino Group Protons in Cations 1, 2, 3, and 5[a]

	$H_{(\alpha\text{-pro-}R)}$	$H_{(\alpha\text{-pro-}S)}$	$H_{(\text{side-pro-}R)}$	$H_{(\text{side-pro-}S)}$
1	[d]	[d]	3.61×10^{-4}	1.35×10^{-3}
2	1.75×10^{-3}	[d]	[b]	4.46×10^{-5}
3	[d]	[d]	2.57×10^{-6}	1.08×10^{-6}
5	2.07×10^{-3}	[d]	[c]	

[a]measured at 300K in 10 mM sodium phosphate buffer, pH* 6.8. [b]The rate of exchange of the side-chain pro-*R* NH proton of **2** cannot be measured because of overlap with the solvent resonance. [c]These protons are not present in **5**. The imidazole NH exchanges with a rate constant >5×10^{-2} s^{-1}. [d]Exchange rates too rapid to be measured by this technique. The fastest exchange rate that can be measured by NMR spectroscopy has been estimated as 5×10^{-2} s^{-1}.

It is striking that the exchange rates vary by over 4 orders of magnitude and that, in some instances, the two protons on the same nitrogen exchange at significantly different rates; for example the pro-*R* and pro-*S* protons of the γ-NH_2 in **1** exchange with 30-fold different rates. This difference in rates for two protons attached to the same coordinating atom suggests that the exchange does not involve breaking of the Ru−N bond.

H−D exchange may occur via an acid- or base-catalyzed mechanism. The acid-catalyzed mechanism would involve ligand dissociation of the amino group as the rate-determining step prior to a rapid H−D exchange, whereas for the base-catalyzed mechanism, deprotonation of the coordinated amino group would be rate-determining. The H−D exchange experiments were carried out in D_2O at pH* 6.8. As such, the base is the solvent, and the observed rate of exchange is expected to be first order for either mechanism. The base-catalyzed mechanism is favored by stronger Ru−N bonds stabilizing the conjugate base, implying a lower energy transition state on achieving the intermediate. Further to this, the acid-catalyzed mechanism would necessitate a highly organized intermediate for the pro-*R* and pro-*S* amino group protons to exhibit the distinct exchange rates that are observed for them.

The decrease in exchange rate as the metallocycle ring size increases is significant, and we believe reflects, paradoxically, a weakening of the side-chain coordination. However, this interpretation is not obvious from the structural data we have gathered thus far, as there does not appear to be a straightforward correlation between optimized ruthenium nitrogen bonding (apparent from the bond lengths and angles observed in the solid-state structures) and faster exchanging NH protons. We do believe that the differences in the observable rates of exchange indicate subtle distinctions in reactivity of the protons and the ruthenium−nitrogen bonds to which they append, and we interpret these in terms of changing pK_a values (see below).

Reaction of Lys·HCl with $[(PhH)RuCl_2]_2$ in the absence of base resulted in crystals of $[\mathbf{8}][SbF_6]$ suitable for X-ray diffraction, showing bidentate lysine chelating $[(PhH)RuCl]^+$ through the carboxylate and α-amino groups (Figure 5).

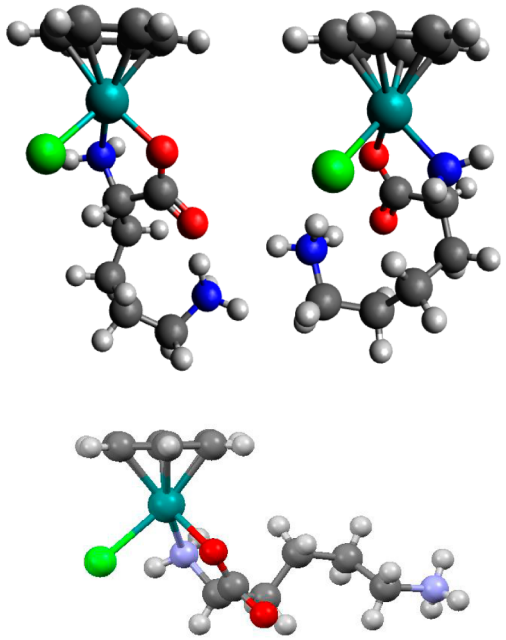

Figure 5. Computed gas-phase structures of **8** (top left), its diastereomer (top right), and the crystallographically obtained structure of **8** for comparison (bottom).

Charge balancing suggests that the side-chain amino group is protonated in this structure. Although there was insufficient material for NMR spectroscopic analysis, ESI-MS gave signals consistent with the composition of the crystal structure. Only one enantiomer was observed in the solid-state. Computation of the respective energies of the different binding modes (Figure 5) suggests that the *in vacuo* energies of the isomers differ by 1.141 kcal/mol, with the stereochemistry found in the solid-state being the more stable. It should be noted, however, that the calculated geometry differed significantly from that found in the crystal structure, apparently favoring internal hydrogen bonding in the absence of the SbF_6^- counterion.

More interesting still, the crystal structure of $[\mathbf{8}][SbF_6]$ suggests that the bidentate binding mode could be favored over the tridentate arrangement by simple protonation of a would-be ligand. The possibility of pH-triggered hemilability was one we found interesting. We reacted one of the tridentate complexes, **1**, with acetic acid in water in an attempt to labilize a donor atom by trapping it with a proton as a pendant conjugate acid. This would allow another Lewis base such as acetate or water to fill the now-vacant site.

In the event, analysis of the reaction mixture by MS suggested that [**1**·HOAc] had formed (as well as [**1**·HCl]); we attribute the presence of chloride to impurities in the solvent.

DOI: 10.1021/ic502051y
Inorg. Chem. 2015, 54, 3118−3124

Consistent with the MS signals, the NMR spectra of the reaction mixture display NOESY cross-peaks between the methyl group of acetic acid and both the β-CH_2 and α-CH signals from the DAP ligand, as well as two new η^6-benzene environments and two new ^{13}C signals in the carbonyl region.

These results show that an "inert" complex could become primed to react by a lowering of pH. This is particularly relevant to medicinal ruthenium research, as cancerous cells are typically more acidic than healthy cells. An acidic pH "trigger" like this could be incorporated into a Ru(II) drug, increasing its specificity. While searching the literature for such reactivity is challenging, we do not believe that such acid-catalyzed hemilability has been reported for small-molecule complexes before, though the behavior is well-known in metalloproteins.

Becoming interested in the potential of $[\mathbf{1}][PF_6]$ to react with biomolecular targets, we attempted to react it with *N*-acetyl methionine methyl ester. This N,O-protected amino acid better mimics methionine in a peptide than the free amino acid, leaving only the soft thioether group as a possible coordination site.

Incubating excess *N*-Ac-Met-OMe with $[\mathbf{1}][PF_6]$ at 40 °C over 6 weeks resulted in a solution whose MS showed a peak due to $[\mathbf{1}{\cdot}N\text{-Ac-Met-OMe}]^+$. The one-dimensional ^1H NMR spectrum showed no new, resolved signals (see Supporting Information section 3), but we believe that this is simply because the product peaks overlap with those of the starting material; the NOESY spectrum indicates through-space coupling between the aliphatic α-CH and β-CH_2 protons on the DAP ligand and the methionine γ-CH_2 group, adjacent to the sulfur atom (see Supporting Information section 3). We do not believe that these cross-peaks can be explained by simple intermolecular interaction: they suggest the formation of a Ru−S bond.

Interestingly, the MS data suggest that the carboxylate ligand has dissociated in preference to the amino group, because the resulting free amine would become rapidly protonated in aqueous acid, and should be seen as a peak due to $[\mathbf{1}\text{-H}]^{2+}$, which is absent from the ESI-MS spectrum. We note that this is consistent with expected Ru−X bond strengths: the soft N center is a better σ-donor than the hard O center. Further, the carboxylate ligand is vulnerable to activation by protonation (Scheme 2) in a way that the coordinatively saturated amine ligand is not: the carbonyl group has multiple lone pairs of electrons which could conceivably act as a Bronsted base, resulting in the decomplexation of the neutral −COOH fragment. Under most pH regimes, this would be then expected to revert to the carboxylate. DFT calculations (see Supporting Information section 5) displaying the forms of the MO (Figure 6) corroborate this: The HOMO of **1** has large, orthogonal orbital coefficients on the oxygen atoms.

Scheme 2. Proposed Mechanism for Acid-Catalyzed Ligand Substitution

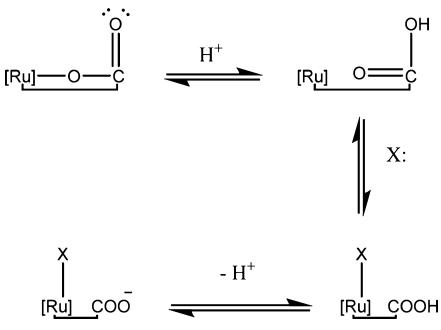

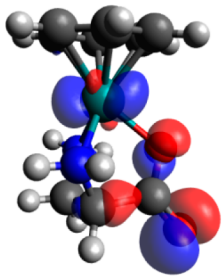

Figure 6. HOMO of **1**. Note the large coefficients on the oxygen atoms, which seem to become labilized in acid in preference to the amino groups.

Noting that this reaction still yielded only a small proportion of $[\mathbf{1}\ N\text{-Ac-met-OMe}]^+$, and that it was extremely slow, we considered how a pH buffer might affect the reactivity. Having already established that acid labilizes the DAP, we incubated $[\mathbf{1}][PF_6]$ with *N*-Ac-met-OMe in acidic buffer.

This reaction was initially followed by MS. Within 2 days, a significant peak due to $[\mathbf{1}{\cdot}N\text{-Ac-Met-OMe}]^+$ was observed at m/z = 488.1 Da (expected 488.08 Da), though **1** was still clearly present. As mentioned above, one-dimensional NMR spectroscopy was difficult to interpret due to signal overlap, but a DOSY spectrum (see Supporting Information Figure 3.2) was consistent with the arene and methionine fragments being present in the same species, a strong indication of covalent bonding between the ruthenium starting material and the protected methionine molecule.

Further, this result indicates that the carboxylate residue (rather than an amine ligand) has been displaced from the metal. Displacement of an amine ligand would yield an ammonium group whose presence would be detected by ESI-MS, but the gain of an additional proton is not observed. Reducing the hapticity of the arene ring seems unlikely to yield a product so stable in aerobic water.

In principle there are two possible stereochemical outcomes at the Ru center from the proposed carboxylate displacement by *N*-Ac-Met-OMe: either with retention or inversion of ruthenium's stereoconfiguration. These possibilities were investigated computationally. The optimized gas-phase structures (Figure 7) differed in energy by only 0.027 kcal/mol, suggesting that product stereocontrol (if any) would be kinetic rather than thermodynamic. Spectroscopy did not show evidence that would distinguish the species (for example, no NOESY cross-peak was observed between the DAP or methionine ligands and the arene ring). Although we remain unsure about the dominant product stereochemistry at Ru, the increased speed and extent of the substitution reaction in the presence of acid is noteworthy.

■ CONCLUSIONS

Controlling the diastereomer formed in reactions between $[(PhH)Ru]^{2+}$ and a tridentate amino acid is quite straightforward, and depends upon the enantiomer of amino acid chosen. In this set of examples, we can see that the ease of synthesis and practical stability of the tridentate complex formed is correlated with the ring size of the resultant metallocycle formed when the side-chain coordinates. From our observations, 5- or 6-membered rings appear relatively easy to synthesize and

DOI: 10.1021/ic502051y
Inorg. Chem. 2015, 54, 3118−3124

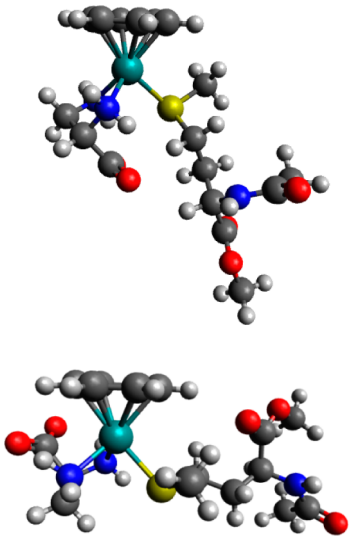

Figure 7. Optimized structures of [**1**·*N*-Ac-met-OMe]$^+$. The bottom structure is more stable by 0.027 kcal/mol.

crystallize readily, while the single example we have of a 7-membered ring has only been characterized in solution by NMR. We can see that with side-chain amino groups as the ligands, varying this ring size from 5 to 8 has dramatic consequences on the stabilities of the complex cations generated, to the point that the 8-membered ring will not stably form.

By definition, coordination of an amino group to the metal lowers the pK_a values of both the protonation of the neutral amino group and for the protonation of a coordinated imido group ($-NH^-$). At pH 7, it is clear that the amino acid side-chains are coordinated as NH_2 but then surprisingly, in the examples shown above, the H/D exchange rates for the two protons on this coordinated amine exchange more slowly than those of the coordinated α amino group protons. In addition, the exchange rate for these side-chain amino group protons decreases as the side-chain gets longer, perhaps indicating that the pK_a values for the side-chain amino groups are being raised back toward their values in the free amino acid. This may indicate weaker bonding of the nitrogen to the metal to the point that, in the tridentate lysine complex, protons compete with the metal for the lysine ϵ amino group and the tridentate complex will not stably form. Lysine is, however, perfectly stable in a bidentate coordinated mode. DAP has been used in a diamino coordinated bidentate mode before.[14]

In the case of DAP the amino acid carboxylate can be protonated and shown to be labile. This suggests that, within the coordinated complex, the apparent pK_a for protonation of this conjugate base must be higher than that for protonation of either the α or β amino groups in this ligand. This lowering of the amino group pK_a values has not been explored before in this context.

We have shown that [(PhH)Ru(amino acid)]$^+$ complexes are relatively stable and long-lived in buffered aqueous solution but could be triggered into ligand exchange in the right environment, which could either be a change in the bulk solution properties (in a specific biological compartment for instance) or by local provision of alternative, strong Lewis basic donor atoms, such as when bound to a specific protein or nucleic acid structure where ligand exchange can be triggered by the structural environment. By appropriate choice of amino acid, one could make either the side-chain ligand or the "main chain" carboxylate the labile ligand.

The acid-triggered lability of the resulting chelates is an extremely interesting feature, and appears particularly relevant to anticancer applications, as it could provide a high degree of selectivity between rates of reaction in healthy and diseased cells. Building upon the synthetic and structural understanding discussed here, we can continue to study the reaction of this suite of complexes with simple and more complex biochemical targets. These pro-complexes may also be of interest to other medicinal applications or as biocompatible catalysts[19] with the potential to provide specificity and enantioselectivity, an attractive behavior in a drug candidate; we hope that the use of these chelates will provide a new strategy in the move away from cisplatin-type lability that is thought to be the origin of highly nonselective binding and general cytotoxicity.

EXPERIMENTAL SECTION

Syntheses. The syntheses of $[(PhH)RuCl_2]_2$, [(PhH)Ru(Aa)]-$[PF_6]$ (Aa = diaminopropionic acid (DAP) [**1**][PF_6], diaminobutanoic acid (DAB) [**2**][PF_6], ornithine [**3**][PF_6], histidine [**5**][PF_6], methionine [**6**][PF_6], aspartic acid [**7**]) as well as that of [(PhH)Ru(Lys-H)(Cl)][SbF_6] ([**8**][SbF_6]) and the attempted synthesis of lysine [**4**][PF_6] are detailed in the Supporting Information. All reagents were used as received. Syntheses involving air- and moisture-sensitive reagents and products were undertaken using the appropriate precautions.

In the representative synthesis of [**1**][PF_6], $[(PhH)RuCl_2]_2$ (149 mg, 0.299 mmol) and 2,3-diaminopropionic acid monohydrochloride (84.9 mg, 0.604 mmol) were dissolved in MeOH (15 mL). Triethylamine (0.08 mL, 0.6 mmol) was added, and the solution stirred overnight at 40 DEG under nitrogen. The solution was filtered, and the filtrate exposed to vacuum at 40 °C until precipitate was observed. NH_4PF_6 (299 mg, 1.83 mmol) was then added, precipitating the product as a yellow solid, which was filtered, washed with ice-cold MeOH, and dried *in vacuo* to give a daffodil-yellow powder (103.8 mg, 0.243 mmol, 40%). Recrystallization from hot MeOH gave needle-like crystals suitable for X-ray diffraction analysis.

Instrumentation. Mass spectrometry was performed on a Micromass Quattro LC ESI-mass spectrometer. Samples were typically prepared in ultrapure water or 50:50 ultrapure water/acetonitrile. Ionization was achieved with a capillary voltage of 2.8 kV, cone voltage of 30 V and a collection voltage of 3 V. Desolvation and capillary temperatures were 40 °C.

^{1}H, ^{13}C, and two-dimensional NMR spectra were collected using a DRX-500 FT-NMR or ATM DPX-400 FT-NMR spectrometer. ^{1}H NMR spectra were collected at 500 and 400 MHz on the respective spectrometers and ^{13}C NMR spectra at 125 MHz.

Data from proton−deuterium exchange experiments were collated and analyzed with Bruker's Dynamic Centre Package. Integrals were normalized relative to the 6H singlet of the benzene ligand (assumed to remain constant). A detailed description of experiments is provided in the Supporting Information.

Single-crystal X-ray diffraction studies were performed at 180 K using a Nonius Kappa CCD. Structures were solved by direct methods, and refinement on F^2 was by full-matrix least-squares techniques.

IR spectra were collected from solids on a PerkinElmer Spectrum TWO FT-IR machine and analyzed using the Spectrum software package.

DFT calculations were performed using the Gaussian09 package.[20] After trialing several different methods (see Supporting Information), we settled on using the B3LYP hybrid functional and the LANL2DZ basis set for Ru and the 6-31G(d,p) basis set for all other elements. We have included a more detailed workflow in the Supporting Information to enable reproducibility, and hope that the wider chemical community will consider sharing workflows in a similar manner.

DOI: 10.1021/ic502051y
Inorg. Chem. 2015, 54, 3118−3124

■ ASSOCIATED CONTENT

Supporting Information

Details of the synthesis of all compounds, NMR analyses, X-ray diffraction and ORTEP diagrams, details of computational methods. Crystallographic data in CIF format. This material is available free of charge via the Internet at http://pubs.acs.org.

■ AUTHOR INFORMATION

Corresponding Authors

*E-mail: srb26@cam.ac.uk.
*E-mail: pdb30@cam.ac.uk.

Present Address

‡H.S. current address is the Chemistry Department, University of Oxford, South Parks Road, Oxford, United Kingdom.

Author Contributions

†The first two authors contributed equally to the work.

Author Contributions

T.G.S., M.J.O., A.J.P., P.W.S., P.D.M., and H.S. designed, performed, and analyzed experiments. M.J.O. carried out DFT calculations. T.G.S. and M.J.O. wrote the initial draft. S.R.B. and P.D.B. designed experiments, analyzed data, and wrote the manuscript. All authors have given approval to the final version of the manuscript.

Funding

T.G.S. and M.J.O. thank the EPSRC for Studentships EP/P505445/1 and EP/K503/009/1, respectively.

Notes

The authors declare no competing financial interest.

■ ACKNOWLEDGMENTS

We thank Dr. Alex Simperler, and the NSCCS training facilities, for assistance with DFT calculations, Duncan Howe, of the Chemistry Department NMR service, Dr. John Davies for crystallographic data collection and refinement, and BP for a summer studentship to H.S.

■ REFERENCES

(1) Nazarov, A. A.; Hartinger, C. G.; Dyson, P. J. *J. Organomet. Chem.* **2014**, *751*, 251−260.
(2) Antonarakis, E. S.; Emadi, A. *Cancer Chemother. Pharmacol.* **2010**, *66*, 1−9.
(3) Smith, G. S.; Therrien, B. *Dalton Trans.* **2011**, *40*, 10793−10800.
(4) Noffke, A. L.; Habtemariam, A.; Pizarro, A. M.; Sadler, P. J. *Chem. Commun.*. **2012**, *48*, 5219−5246.
(5) Groessl, M.; Hartinger, C. G. *Anal. Bioanal. Chem.* **2013**, *405*, 1791−1808.
(6) Wills, R. H.; Habtemariam, A.; Lopez-Clavijo, A. F.; Barrow, M. P.; Sadler, P. J.; O'Connor, P. B. *J. Am. Soc. Mass Spectrom.* **2014**, *25*, 662−672.
(7) Wolters, D. a; Stefanopoulou, M.; Dyson, P. J.; Groessl, M. *Metallomics* **2012**, *4*, 1185−1196.
(8) Will, J.; Sheldrick, W. S.; Wolters, D. *JBIC, J. Biol. Inorg. Chem.* **2008**, *13*, 421−434.
(9) Maksimoska, J.; Feng, L.; Harms, K.; Yi, C.; Kissil, J.; Marmorstein, R.; Meggers, E. *J. Am. Chem. Soc.* **2008**, *130*, 15764−15765.
(10) Bruijnincx, P. C. A.; Sadler, P. J. *Curr. Opin. Chem. Biol.* **2008**, *12*, 197−206.
(11) Habtemariam, A.; Melchart, M.; Fernández, R.; Parsons, S.; Oswald, I. D. H.; Parkin, A.; Fabbiani, F. P. A.; Davidson, J. E.; Dawson, A.; Aird, R. E.; Jodrell, D. I.; Sadler, P. J. *J. Med. Chem.* **2006**, *49*, 6858−6868.
(12) Morris, R. E.; Aird, R. E.; Murdoch, P. D. S.; Chen, H.; Cummings, J.; Hughes, N. D.; Parsons, S.; Parkin, A.; Boyd, G.; Jodrell, D. I.; Sadler, P. J. *J. Med. Chem.* **2001**, *44*, 3616−3621.
(13) Scolaro, C.; Bergamo, A.; Brescacin, L.; Delfino, R.; Cocchietto, M.; Laurenczy, G.; Geldbach, T. J.; Sava, G.; Dyson, P. J. *J. Med. Chem.* **2005**, *48*, 4161−4171.
(14) Barragán, F.; Carrion-Salip, D.; Gómez-Pinto, I.; González-Cantó, A.; Sadler, P. J.; de Llorens, R.; Moreno, V.; González, C.; Massaguer, A.; Marchán, V. *Bioconjugate Chem.* **2012**, *23*, 1838−1855.
(15) Bíró, L.; Balogh, E.; Buglyó, P. *J. Organomet. Chem.* **2013**, *734*, 61−68.
(16) Egbewande, F. A.; Paul, L. E. H.; Therrien, B.; Furrer, J. *Eur. J. Inorg. Chem.* **2014**, *2014*, 1174−1184.
(17) Melchart, M.; Habtemariam, A.; Novakova, O.; Moggach, S. A.; Fabbiani, F. P. A.; Parsons, S.; Brabec, V.; Sadler, P. J. *Inorg. Chem.* **2007**, *46*, 8950−8962.
(18) Reiner, T.; Jantke, D.; Miao, X.-H.; Marziale, A. N.; Kiefer, F. J.; Eppinger, J. *Dalton Trans.* **2013**, *42*, 8692−8703.
(19) Dougan, S. J.; Habtemariam, A.; McHale, S. E.; Parsons, S.; Sadler, P. J. *Proc. Natl. Acad. Sci. U.S.A.* **2008**, *105*, 11628−11633.
(20) Frisch, M. J.; Trucks, G. W.; Schlegel, H. B.; Scuseria, G. E.; Robb, M. A.; Cheeseman, J. R.; Scalmani, G.; Barone, V.; Mennucci, B.; Petersson, G. A.; Nakatsuji, H.; Caricato, M.; Li, X.; Hratchian, H. P.; Izmaylov, A. F.; Bloino, J.; Zheng, G.; Sonnenberg, J. L.; Hada, M.; Ehara, M.; Toyota, K.; Fukuda, R.; Hasegawa, J.; Ishida, M.; Nakajima, T.; Honda, Y.; Kitao, O.; Nakai, H.; Vreven, T.; Montgomery, J. A., Jr.; Peralta, J. E.; Ogliaro, F.; Bearpark, M.; Heyd, J. J.; Brothers, E.; Kudin, K. N.; Staroverov, V. N.; Kobayashi, R.; Normand, J.; Raghavachari, K.; Rendell, A.; Burant, J. C.; Iyengar, S. S.; Tomasi, J.; Cossi, M.; Rega, N.; Millam, M. J.; Klene, M.; Knox, J. E.; Cross, J. B.; Bakken, V.; Adamo, C.; Jaramillo, J.; Gomperts, R.; Stratmann, R. E.; Yazyev, O.; Austin, A. J.; Cammi, R.; Pomelli, C.; Ochterski, J. W.; Martin, R. L.; Morokuma, K.; Zakrzewski, V. G.; Voth, G. A.; Salvador, P.; Dannenberg, J. J.; Dapprich, S.; Daniels, A. D.; Farkas, Ö.; Foresman, J. B.; Ortiz, J. V.; Cioslowski, J.; Fox, D. J. *Gaussian 09, Revision D.01*; 2009.

DOI: 10.1021/ic502051y
Inorg. Chem. 2015, 54, 3118−3124